

# Theoretical Bounds on Random Errors in Satellite Doppler Navigation

NADAV LEVANON, Senior Member, IEEE  
Tel-Aviv University

**Analytic expressions of the random errors in a satellite Doppler navigation system are developed. The errors in the along-track and across-track coordinates are expressed as functions of the geometry (range and angle), pass-length, and signal-to-noise ratio (SNR). Such an analytic result becomes possible due to an explicit solution to a simplified rectilinear model of the satellite pass over a flat Earth. It is shown that the explicit solution performance in the presence of noise is identical to that of the iterative solution, used in the real navigation problem.**

## I. INTRODUCTION

Satellite Doppler navigation, developed between 1957 and 1963 [1] at the Applied Physics Laboratory of Johns Hopkins University, is presently in wide global use. At least three different satellite systems provide Doppler navigation: 1) the U.S. Navy TRANSIT system, which is also used extensively for civilian marine navigation, geodesy and surveying; 2) the French ARGOS system, on board the U.S. TIROS satellites, which is used for location of unmanned environmental platforms; and 3) the Search and Rescue satellites Sarsat and COSPAS, which locate beacons transmitting distress messages.

Analytical analysis of the system performance is hampered by the nonlinear nature of the problem. Solving for the position is obtained iteratively by a least squares technique which produces the position that minimizes the difference between the expected and the measured Doppler history. Most of the accuracy evaluations have been based on numerical simulation.

Two questions are addressed by an analytical error analysis of the system: 1) what is the dependence of the random position error on the signal-to-noise ratio (SNR), and 2) what is the contribution of various sections and lengths of the satellite track to the position accuracy? Following the practice in TRANSIT [2] it is assumed that Doppler cycle count, rather than Doppler frequency, is being measured, and that the system estimates three parameters: latitude, longitude, and the wavelength of the transmitted navigation signal. In practice the third unknown is the frequency of the oscillator in the navigated platform, or the difference between it and the satellite frequency. Choosing the wavelength of the transmitted signal is a convenient representation of this third unknown.

To be able to answer these questions analytically, a simple model of the satellite navigation problem will be developed, in which the navigation fix can be solved explicitly. The explicit solution lends itself to an analytic error analysis. The simple model and the explicit solution cannot be used in real life because they do not readily accept the many inputs and corrections that the iterative solution can handle. However, the model is adequate for error analysis. It is shown that the error analysis applies to the iterative solution.

The error analysis is based on the Cramer-Rao lower bound on the random error. It is a practical bound for this application, because the Doppler navigation system operates at a very high SNR and with very small errors.

This paper relies heavily on a previous paper [3] in which a similar problem was treated. Derivations leading to some of the results are outlined there and are not repeated here.

## II. THE MODEL

The elliptical satellite orbit over a rotating oblate Earth will be replaced by the most simple model possible,

Manuscript received Feb. 29, 1984.

Author's address: Department of Electronic Systems, Tel-Aviv University, Tel-Aviv 69978, Israel.

0018-9251/84/1100-0810 \$1.00 © 1984 IEEE

that of uniform rectilinear motion, at a fixed height, over a stationary flat Earth (Fig. 1). The a-priori knowledge of the satellite orbit is, consequently, expressed by a given

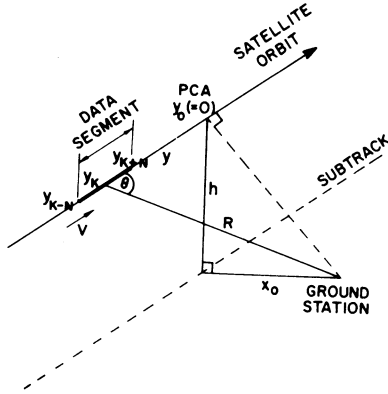


Fig. 1. Relative geometry between satellite pass and ground station, in simplified model.

height  $h$ , a given constant velocity  $V$ , and a given satellite position along the track  $y_0$ , at a given time  $t_0$ .  $y$  will be the axis along the track, and  $x$  across the track. The fix is the position of the stationary ground station relative to the satellite position at  $t_0$ , hence the fix is  $(x_0, y_0)$ . The position of the satellite along the track at time  $t_k$  is given by

$$y_k = y_0 + V(t_k - t_0). \quad (1)$$

Note that as plotted in Fig. 1,  $y_0 = 0$  and  $y_k$  is negative. This arbitrary but convenient choice does not affect the generality of the analysis.

It should be pointed out that by giving up the Earth rotation, it becomes impossible to distinguish between symmetrical fixes on either side of the orbit plane.

### III. THE EXPLICIT SOLUTION

The explicit solution is based on parameterizing the one-way signal phase by Taylor series expansion around the center of the observation period  $t_k$ .

$$\Phi_s(t_k + t) = b_0 + b_1 t + b_2 t^2 + b_3 t^3 + \Phi_E(t) \quad (2)$$

where  $b_0, b_1, b_2$ , and  $b_3$  are functions of  $t_k$ , and where  $\Phi_E$  represents the remaining terms.

There is a simple relation between  $b_1, b_2$ , and  $b_3$ , and the range rate and its two derivatives at the corresponding instant. The  $n$ th derivative of  $R$  with respect to time is given by

$$R^{(n)} = \lambda n! b_n / 2\pi, \quad n = 1, 2, \dots \quad (3)$$

where  $\lambda$  is the unknown wavelength.

With  $\Theta$  and  $R$  as defined in Fig. 1 the range derivatives can be expressed as functions of  $\Theta, R$ , and  $V$ . The first five derivatives are given below:

$$R^{(1)} = -V \cos \Theta \quad (4)$$

$$R^{(2)} = V^2 \sin^2 \Theta / R \quad (5)$$

$$R^{(3)} = 3 V^3 \sin^2 \Theta \cos \Theta / R^2 \quad (6)$$

$$R^{(4)} = (3 V^4 / R^3) \sin^2 \Theta (5 \cos^2 \Theta - 1) \quad (7)$$

$$R^{(5)} = (15 V^5 / R^4) \sin^2 \Theta \cos \Theta (4 - 7 \sin^2 \Theta). \quad (8)$$

Using (3)–(6) and some simple geometry, it can be shown that the three unknowns  $x_0, y_0$ , and  $\lambda$ , are given by

$$y_0 = V(2b_2/b_1 - b_3/b_2)^{-1} - V(t_k - t_0) \quad (9)$$

$$x_0 = [-(b_1 b_3 / b_2^2 - 2)^{-2} 2V^2 b_1 / b_3 - h^2]^{1/2} \quad (10)$$

$$\lambda = 2\pi V(b_1^2 - 2b_1 b_2^2 / b_3)^{-1/2}. \quad (11)$$

Note that for three unknowns, three measurable range derivatives were needed,  $R^{(1)}, R^{(2)}$ , and  $R^{(3)}$ . (In a narrowband Doppler system the range itself  $R^{(0)}$  is not measurable.) If there were more unknowns, such as a frequency drift, then higher range derivatives would have been required.

One interesting result from (9) and (10) is the coupling of an error in  $h$  to an error in the across-track ( $x$ ) coordinate of the fix, but not to an error in the along-track coordinate. Users of satellite Doppler navigation are usually aware of the fact that entering an erroneous altitude input will cause an error mainly in longitude. Since the satellite orbit is nearly polar, an across-track error is almost equivalent to an error in longitude.

### IV. THE MEASUREMENT SCHEME

In [3] it was shown that the optimal way to estimate the coefficients of the phase polynomial is by using the ‘‘Doppler count’’ measurement. The optimal scheme requires continuous monitoring of the signal during the entire observation period. The phase difference relative to the phase at a reference time (any time during the observation period, and typically at its center or its beginning) is measured unambiguously by counting the number of Doppler cycles which occurred since the reference time mark. (To guarantee enough cycles between intervals, even at low or zero Doppler, the practice is to operate the ground platform at some offset frequency from the satellite frequency.)

To reduce the number of subscripts, let the reference time be at the middle of the observation period,  $t_k$ . Then the phase difference at time  $t_i$  is a function of the number of Doppler counts,  $n_i$ , which occurred since  $t_k$ ,

$$\Phi(t_i) - \Phi(t_k) = 2\pi n_i. \quad (12)$$

Because of additive noise the received phase  $\Phi_R(t)$  is given by

$$\Phi_R(t) = \Phi_S(t) + \Phi_N(t) \quad (13)$$

where  $\Phi_S(t)$  is the noise-free signal phase defined in (2), and  $\Phi_N(t)$  is a zero-mean, phase component resulting from the additive noise.

Our task is to estimate the parameters  $b_1$ ,  $b_2$ , and  $b_3$  in (2), from  $\emptyset_R(t)$ . The additive noise  $\emptyset_N(t)$  will be the source of a random error. The remainder of the Taylor expansion  $\emptyset_E(t)$  will be the source of a bias error if ignored. However, the two errors are not independent quantities. If  $b_1$ ,  $b_2$ , and  $b_3$  are estimated assuming (contrary to fact)  $b_4 = b_5 = \dots = 0$ , then the result is more biased but the sensitivity to noise is smaller than if the higher coefficients are considered.

Due to the assumption of high SNR (small error), it is possible to circumvent that tradeoff. First,  $b_1$ ,  $b_2$ , and  $b_3$  will be estimated while ignoring the higher coefficients. These three parameters, slightly biased, allow solving for a slightly biased fix, using (9), (10), and (11). Once the geometry is known,  $b_4$ ,  $b_5$ , and the bias error that resulted from ignoring them, can be calculated and subtracted, to yield an almost bias free fix. This scheme was developed in [3].

The least squares estimate of the coefficients  $b_1$ ,  $b_2$ , and  $b_3$  will be considerably simplified if the data set consists of an odd number of equally spaced phase difference measurements

$$d\emptyset_j = \emptyset_R(t_i) - \emptyset_R(t_k) \quad (14)$$

where

$$j = i - k = 0, \pm 1, \pm 2, \dots, \pm N \quad (15)$$

and where

$$t_i - t_{i-1} = dt. \quad (16)$$

In that case and ignoring  $b_4$ ,  $b_5$ , ..., the estimated coefficients for each  $k$  are given by

$$b_1 = (dt)^{-1} (P_2 P_6 - P_4^2)^{-1} (P_6 \sum_{j=-N}^N j d\emptyset_j - P_4 \sum_{j=-N}^N j^3 d\emptyset_j) \quad (17)$$

$$b_2 = (dt)^{-2} (P_0 P_4 - P_2^2)^{-1} (P_0 \sum_{j=-N}^N j^2 d\emptyset_j - P_2 \sum_{j=-N}^N d\emptyset_j) \quad (18)$$

$$b_3 = (dt)^{-3} (P_2 P_6 - P_4^2)^{-1} (P_2 \sum_{j=-N}^N j^3 d\emptyset_j - P_4 \sum_{j=-N}^N j d\emptyset_j) \quad (19)$$

where

$$P_m = \sum_{j=-N}^N j^m \quad (20)$$

or specifically

$$P_0 = 2N + 1 \quad (21)$$

$$P_2 = (2N^3 + 3N^2 + N)/3 \quad (22)$$

$$P_4 = P_2(3N^2 + 3N - 1)/5 \quad (23)$$

$$P_6 = P_2(3N^4 + 6N^3 - 3N + 1)/7. \quad (24)$$

## V. BIAS ERROR

Using (17)–(19) in (9)–(11) yields a slightly biased estimate of the ground station position. The sensitivity to noise will decrease, but the bias error will increase, as the length of the satellite pass (used for estimating  $b_1$ ,  $b_2$ , and  $b_3$ ) will increase. Utilizing an analysis similar to the one given in [3, Sec. III] we obtain explicit expressions for the bias errors in  $y_0$  and  $x_0$ . The expressions are functions of  $\sin^2\Theta$ ,  $\cos^2\Theta$ , and the total observation time  $T$ , which are given by

$$\sin^2\Theta = (1 - b_1 b_3 / 2b_2^2)^{-1} \quad (25)$$

$$\cos^2\Theta = (1 - 2b_2^2 / b_1 b_3)^{-1} \quad (26)$$

$$T = 2N dt. \quad (27)$$

The symbol  $\Theta$  is the same angle as defined in Fig. 1, namely, the angle between the velocity and the slant range at the center of the data segment.

The two expressions for the bias errors are

$$dy = (1/504) (27\sin^2\Theta - 32\cos^2\Theta - 25\sin^2\Theta \cos^2\Theta) \times (VT \cos\Theta)^2 / [y_0 + V(t_k - t_0)] \quad (28)$$

and

$$dx = [(3/7)\cos^2\Theta (5\cos^2\Theta - 1) + (5/36) (1 + 2\cos^2\Theta) (7\sin^2\Theta - 4)] \times (VT \sin\Theta)^2 / 4x_0. \quad (29)$$

The unbiased estimates are therefore

$$y_0 \text{ unbiased} = y_0 - dy \quad (30)$$

and

$$x_0 \text{ unbiased} = x_0 - dx \quad (31)$$

where  $y_0$  and  $x_0$  are obtained from (9) and (10) using the estimated  $b$ s, given by (17)–(19).

To demonstrate the validity of the bias correction scheme, a computer simulation was performed in which phase data was generated for a given geometry. (See (A1) and (A2) in Appendix A, regarding phase data.) This noise-free phase data was then used to calculate the biased and unbiased estimates of  $y_0$  and  $x_0$ . The results are given in Fig. 2. In this specific simulation the parameters were:  $h = 1000$  km,  $x_0 = 1000$  km,  $V = 10$  km/s,  $dt = 0.1$  s,  $\lambda = 1$  m, and  $N = 100$ . The length of the satellite orbit segment  $L$  which was used for each evaluation of the fix, is given by

$$L = 2N V dt \quad (32)$$

which, in this case, is 200 km long. The quantity shown on the horizontal axis is the displacement of the center of

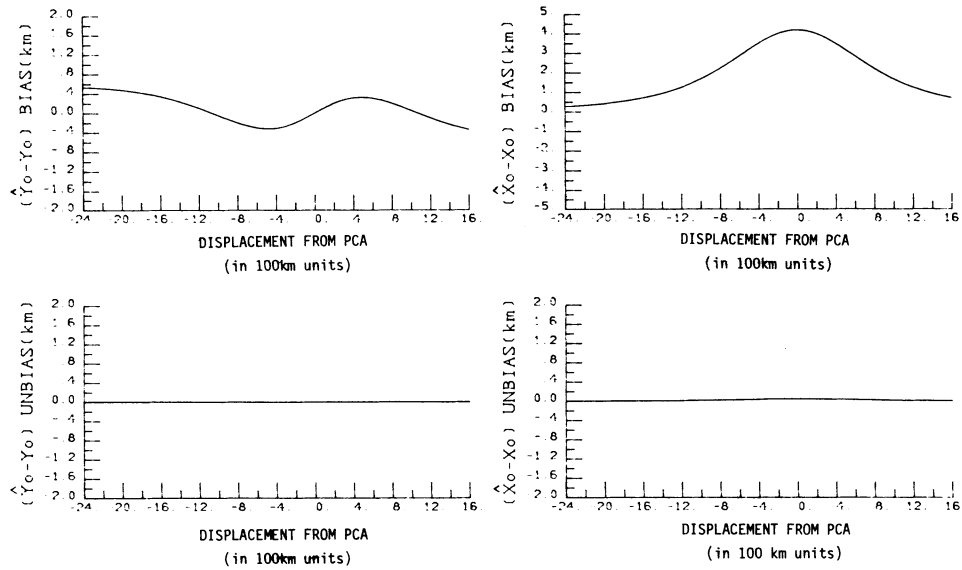


Fig. 2. Bias error before (upper pair) and after (lower pair) bias removal, in along-track (left pair) and across-track (right pair) coordinates.

$L$  since passing the point of closest approach (PCA). It is given in units of 100 km. The quantity on the vertical scale is the bias error in km. The two upper curves show the bias errors of  $y_0$  and  $x_0$  prior to bias correction. (Note that the scale for the bias error in  $x_0$  is from  $-5$  to  $+5$  km, while in all the other curves it is from  $-2$  to  $+2$  km.) The lower pair was obtained after the bias correction. The almost complete removal of the bias error, demonstrates the validity of the assumption that it was caused by ignoring  $b_4$  and  $b_5$ , and the correctness of (28) and (29).

It should be pointed out that the same noise-free phase data was used to solve for the position, utilizing an iterative algorithm. As expected, there was no bias error, and the corresponding curves were perfect straight lines. The iterative algorithm is outlined in Appendix A.

## VI. RANDOM ERROR

To complete the demonstration that the explicit solution and the iterative solution give equal results, it is necessary to compare their performance when the phase data is noisy. The computer simulation was modified and Gaussian noise was added to the generated phase data. The same data, which will be termed “measured phase,” was then used with both the iterative and the explicit solutions. Fig. 3 presents the results of the two solutions when the standard deviation of the phase noise (expressed in units of range) was  $\sigma_R = 0.01$  m. The remaining parameters have not been changed. The definition of the horizontal axis is the same as in Fig. 2. The upper pair presents the errors of the iterative solution, and the lower pair, the explicit solution. The left pair presents the errors along the track, and the right pair, across the track.

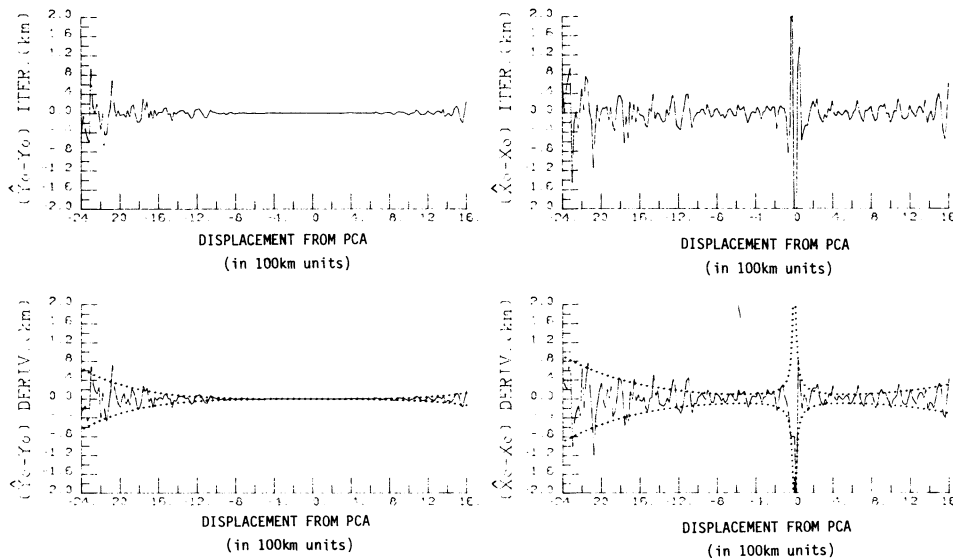


Fig. 3. Position errors in simulation runs with range noise of  $\sigma_R = 0.01$  m. Upper pair obtained with iterative solution. Lower pair obtained with the explicit solution. Dotted lines represent theoretical bounds of the rms errors, as given in (33) and (34).

Fig. 3 reveals 1) the error level and pattern are the same in the iterative approach and in the explicit (derivatives) approach, 2) the errors in the across-track ( $x$ ) direction are larger than in the along-track ( $y$ ) direction, 3) the error in the  $y$  direction decreases as the satellite pass segment, used for navigation, is closer to the PCA, and 4) in the  $x$  direction, the error decreases as the observation segment approaches the PCA, but near the PCA the sensitivity to noise peaks up again.

Having demonstrated the identical performance of the iterative and explicit solutions in the presence of noise, we will now present an analytic expression for the random error effect in the explicit solution, and claim that it applies also to the iterative solution.

The random error analysis follows the analysis in [3, Section V] and will not be repeated here. The final expressions for the root-mean-square (RMS) errors in the  $y$  and  $x$  directions are

$$\sigma_y = (R/VT) \{ (15/4) \sin^4 \Theta + 12(y/VT)^2 [3(1/\sin^2 \Theta - 2)^2 - 7] + 560(y/VT)^4 / \sin^4 \Theta \}^{1/2} (5N_0/A^2 T)^{1/2} \lambda / 2\pi \quad (33)$$

$$\sigma_x = 2(R^2/x_0 VT \cos \Theta) \{ (15/4) [\sin^2 \Theta (2 \cos^2 \Theta - \sin^2 \Theta)]^2 + (R/VT)^2 [36 \cos^6 \Theta + 21 \sin^2 \Theta (6 \cos^4 \Theta - \sin^2 \Theta \cos^2 \Theta - \sin^4 \Theta)] + 35(R/VT)^4 (1 + 2 \cos^2 \Theta)^2 \}^{1/2} \times (5N_0/A^2 T)^{1/2} \lambda / 2\pi. \quad (34)$$

The distance from the center of the observation section to the PCA is  $y = R \cos \Theta$ ,  $N_0$  is the noise spectral level, and  $A$  is the amplitude of the received signal. Note that  $(N_0/A^2 T)^{1/2}$  is the effective SNR. Recall that  $VT$  is the length of the satellite pass during the observation period, and  $R$  is the range from the center of that pass section to the navigating ground station.

In Appendix B it is shown that the relation between the SNR and the range noise  $\sigma_R$  is given by

$$(N_0/A^2 T)^{1/2} = (2\pi\sigma_R/\lambda) (2N)^{-1/2}. \quad (35)$$

The same  $\sigma_R = 0.01$  m, which was used for the simulation in Fig. 3, was used in (35) to yield the SNR which was then used in (33) and (34). The results were superimposed as dotted lines on the lower pair of curves in Fig. 3. The good agreement between the calculated  $\sigma_y$

and  $\sigma_x$  and the actual random errors, demonstrates clearly the validity of (33) and (34).

In the numerical examples above, the orbit segment used for each calculation of the fix was only 200 km. This is a small segment compared to the prevailing practice of using the entire available pass as one segment. However, equations (33) and (34) are general and any segment length ( $VT$ ) can be used. By using a small orbital segment and shifting its displacement from the PCA, we were able to show the relative importance of different sections of the pass to the fix accuracy. From Fig. 3 it is obvious that the most valuable orbital segment, with regard to the along-track error, is the segment centered at the PCA. On the other hand, an orbit segment somewhat off the PCA is the most valuable one as far as across-track error is concerned.

To get a better insight on the behavior of  $\sigma_y$  and  $\sigma_x$ , plots of  $10 \log \sigma_y$  and  $10 \log \sigma_x$ , using (33) and (34), are given in Fig. 4. They were generated using the same parameters as the previous figures, except that it is assumed that  $5N_0\lambda^2/A^2 T 4\pi^2 = 1 \text{ m}^2$ , and the vertical scale is in dB above 1 m. It is interesting to note that with the given geometry the error in  $x$  is always larger than the error in  $y$ , with the ratio of errors reaching a maximum when the observation section is centered around the PCA. To show the effect of increasing the length of the data segment ( $VT$ ), additional plots were included which correspond to a data segment of 1000 km.

The above discussion has established that (33) and (34) constitute a true measure of the random error performance of a satellite Doppler navigation system, in which the unknowns are the two position coordinates and the wavelength.

## VII. CONCLUSIONS

The main results of this paper are (33) and (34). They are analytic expressions of the random error in the along-track and across-track coordinates of the fix in a satellite Doppler navigation system. The analytic results were obtained for an explicit solution (9)–(11) to a rectilinear model of the satellite motion over a flat Earth. It is shown by simulation that the explicit solution performance, in the presence of noise, is identical to that of the iterative solution, and both agree with the analytic error analysis.

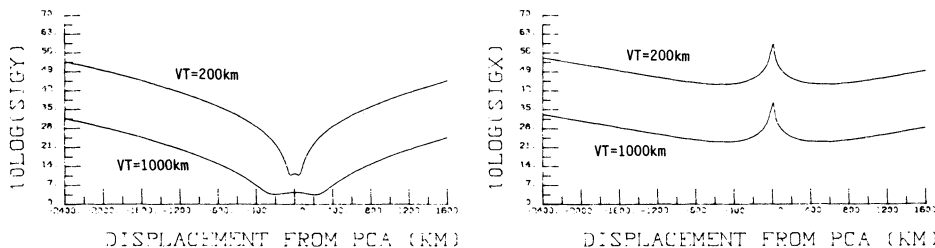


Fig. 4. Plot of (33) and (34) on a logarithmic vertical scale.

An optimal phase measuring scheme was assumed, which makes the result a lower bound on the random error. The Doppler count scheme used in modern TRANSIT receivers is equivalent to the optimal phase measurement, provided that the receiver bandwidth, prior to the phase sampling stage, is matched to the phase sampling interval.

This paper deals with the common surface navigation problem where there are three unknowns, two horizontal coordinates and the exact radio frequency (or wavelength). Additional unknowns to be estimated, such as a frequency drift, or an altitude, would make the system more sensitive to noise. The exact effect can be a subject of a further investigation. Another topic is an analysis of a system which does not provide continuous signal; such a system must utilize Doppler frequency rather than Doppler count. Intermittent signal is typical of systems in which the ground stations transmit and the satellite receives. Since there are many ground stations, each one must transmit at a very low duty cycle, to minimize interference at the satellite receiver. Both ARGOS and SARSAT operate in this mode, and their growing usage makes such an analysis worthwhile.

## APPENDIX A. THE ITERATIVE SOLUTION

The appendix outlines the iterative algorithm against which the explicit (derivatives) solution was tested. The algorithm follows a least-squares Newton approach. Note from Fig. 1 that the range  $R_i$  at time  $t_i$  is given by

$$R_i^2 = x_0^2 + h^2 + [y_0 + V(t_i - t_0)]^2. \quad (A1)$$

The phase at that time is given by

$$\Phi_i = \Phi_c - 2\pi R_i / \lambda \quad (A2)$$

where  $\Phi_c$  is some arbitrary reference phase.

The vector of unknowns is

$$\mathbf{U} = (y_0, x_0, \lambda)^\top. \quad (A3)$$

The phase derivatives with respect to the three unknowns are

$$d\Phi_i / dy_0 = -2\pi [y_0 + V(t_i - t_0)] / \lambda R_i \quad (A4)$$

$$d\Phi_i / dx_0 = -2\pi x_0 / \lambda R_i \quad (A5)$$

and

$$d\Phi_i / d\lambda = 2\pi R_i / \lambda^2. \quad (A6)$$

A Doppler count measuring system deals with phase differences  $\Phi_i - \Phi_k$ , where  $t_k$  was arbitrarily selected at the center of the observation period.

Define the difference partial derivatives,

$$\Phi_{ik}^y = d\Phi_i / dy_0 - d\Phi_k / dy_0 \quad (A7)$$

$$\Phi_{ik}^x = d\Phi_i / dx_0 - d\Phi_k / dx_0 \quad (A8)$$

$$\Phi_{ik}^\lambda = d\Phi_i / d\lambda - d\Phi_k / d\lambda \quad (A9)$$

and the matrix of partial derivatives

$$\mathbf{A} = \begin{bmatrix} \sum_{i=k-N}^{k+N} (\Phi_{ik}^y)^2 & \Sigma(\Phi_{ik}^y \Phi_{ik}^x) & \Sigma(\Phi_{ik}^y \Phi_{ik}^\lambda) \\ \Sigma(\Phi_{ik}^x \Phi_{ik}^y) & \Sigma(\Phi_{ik}^x)^2 & \Sigma(\Phi_{ik}^x \Phi_{ik}^\lambda) \\ \Sigma(\Phi_{ik}^\lambda \Phi_{ik}^y) & \Sigma(\Phi_{ik}^\lambda \Phi_{ik}^x) & \Sigma(\Phi_{ik}^\lambda)^2 \end{bmatrix}. \quad (A10)$$

The iterative algorithm starts with a first guess of the vector of unknowns  $\mathbf{U}$ . Equations (A1), (A2), and the first guess are used to obtain (for each  $k$ )  $2N + 1$   $\Phi_i$ s and one  $\Phi_k$ . Those are compared to the corresponding measured phase differences between the  $t_i$  time marks and  $t_k$ . For each  $i$  the residual phase difference is defined as

$$e_{ik} = \Phi_i^{\text{measured}} - \Phi_k^{\text{measured}} - (\Phi_i - \Phi_k). \quad (A11)$$

Now define a vector  $\mathbf{E}$ ,

$$\mathbf{E} = (E_y, E_x, E_\lambda)^\top \quad (A12)$$

where

$$E_y = \sum_{i=k-N}^{k+N} (\Phi_{ik}^y e_{ik}) \quad (A13)$$

$$E_x = \Sigma(\Phi_{ik}^x e_{ik}) \quad (A14)$$

and

$$E_\lambda = \Sigma(\Phi_{ik}^\lambda e_{ik}). \quad (A15)$$

Then the vector of the next iteration steps  $\mathbf{D}$

$$\mathbf{D} = (D_y, D_x, D_\lambda)^\top \quad (A16)$$

is given by the matrix equation

$$\mathbf{D} = \mathbf{A}^{-1} \mathbf{E} \quad (A17)$$

and the next guess is

$$\mathbf{U} = \mathbf{U} + \mathbf{D}. \quad (A18)$$

After each iteration the magnitude of the position step is compared to an acceptable position error  $d_{\max}$  and if

$$(D_y^2 + D_x^2)^{1/2} \leq d_{\max} \quad (A19)$$

then the iterations are terminated, and the last guess is accepted as the result. Experience shows that with a reasonable  $d_{\max}$ , less than five iterations are usually necessary.

## APPENDIX B. THE RELATION BETWEEN SNR AND $\sigma_R$

It will be assumed that the receiver additive noise is a sample function from a zero-mean Gaussian random process whose power is equally distributed over the receiver frequency band of  $W$  hertz, centered about the signal frequency.

Consider all Nyquist rate samples ( $dt = 1/W$  s) of the observed phase difference. For high SNR conditions, the noise component of the phase samples  $\Phi_N(t_i)$  are

statistically uncorrelated zero-mean random variables whose variance is given by

$$E\{\phi_N^2(t_i)\} = WN_0/A^2. \quad (\text{B1})$$

Here  $N_0/2$  is the (two-sided) noise spectral level and  $A$  is the amplitude of the received signal. The right hand side of (B1) is the ratio of the average noise power to the signal power, prior to the phase sampling operation.

Multiplying and dividing by  $W$  yield

$$N_0/A^2T = (N_0W/A^2)(WT)^{-1}. \quad (\text{B2})$$

The Nyquist rate and (27) yield

$$W = 1/dt = 2N/T \quad (\text{B3})$$

and (3) gives

$$\sigma_R = \lambda \sigma_0/2\pi. \quad (\text{B4})$$

Equations (B1)–(B4) yield the relation between the effective SNR and the equivalent range noise  $\sigma_R$ ,

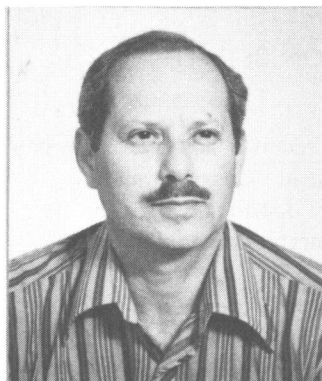
$$N_0/A^2T = (2\pi\sigma_R/\lambda)^2 (2N)^{-1}. \quad (\text{B5})$$

Note that if there were fewer samples during  $T$  (smaller  $N$ ), this would have implied longer intervals  $dt$ , and therefore narrower receiver bandwidth  $W$ . Then, from (B1) and (B4), the equivalent range noise of each measurement would have decreased.

In other words, the performance of the measurement scheme is independent of the number  $2N$  of the  $dt$  intervals, and depends only on their product, the total observation time  $T$ , provided that the receiver bandwidth is kept matched to the phase sampling interval ( $W = 1/dt$ ). However, the algorithm outlined in (17)–(19) becomes somewhat inferior to the optimal estimator if  $N$  is chosen too small.

#### REFERENCES

- [1] Guier, W.H., and Weiffenbach, G.C. (1960) A satellite Doppler navigation system. *Proceedings of the IRE*, 9 (Apr. 1960), 507–516.
- [2] Stansell, T.A. (1976) Positioning by satellites. In S.H. Laurila (Ed.) *Electronic Surveying and Navigation*. New York: Wiley, 1976, ch. 28.
- [3] Levanon, N., and Weinstein, E. (1983) Angle-independent Doppler velocity measurement. *IEEE Transactions on Aerospace and Electronic Systems*, AES-19, 3 (May 1983), 354–359.



**Nadav Levanon** (S'67—M'69—SM'83) was born in Tel-Aviv, Israel, in 1940. He received the B.Sc. and M.Sc. degrees in electrical engineering from the Technion-Israel Institute of Technology in 1961 and 1966, respectively, and the Ph.D. in electrical engineering from The University of Wisconsin, Madison, in 1969.

He is currently an Associate Professor and head of the Department of Electronic Systems at Tel-Aviv University, Tel-Aviv, Israel. He joined Tel-Aviv University in 1970 as a lecturer in the Department of Geophysics. He was a Visiting Associate Professor at The University of Wisconsin, Madison, from 1972 to 1974, and a Visiting Scientist at The Johns Hopkins University/Applied Physics Laboratory, during the 1983/1984 academic year.

Dr. Levanon is a member of the American Meteorological Society, and the American Geophysical Union.